Investigating the Weight Effects on Action Potential Parameters for Simulated Spinal Cord Compression Using Lumbricus Terrestris

Aiden Kim
Peddie School

ABSTRACT

Spinal cord compression is formed by a malignant tumor-generated pressure on the spinal cord. The compression may be initiated anywhere around the spinal cord. Spinal cord compression may be generated by other pathological conditions that bring pressure on the spinal cord, i.e., in case the vertebrae are physically damaged or pressed. Back pain is also sustained throughout the leg area for general complaints. Despite these serious issues, not many animal models have been established. This study investigated the impact on evoked action potential (AP) parameters such as response duration (RD), peak potential (PP), action potential width (APW), and nadir potential (NP) to examine any functional relationship for the standard weights placed on *Lumbricus terrestris*' body. The compression of *Lumbricus terrestris*' spinal cord by weight standards simulated growing tumors in a confined spinal space, and the AP parameters monitored with administration of Tylenol, alcohol and caffeine solution. The study concluded that RP and NP were positively correlated, while PP and EPW were negatively correlated ($P<0.05$) for the weight change. Moderate changes were evident for all the parameters from the weight load on the spine. RD and APW showed approximately 30% more changes caused compared to the NP and PP when injected with the drug solutions. Further study might be continued to expound on detailed underlying mechanisms of the parameter profiles.

TABLE OF CONTENTS

1. INTRODUCTION

Spinal cord compression can be brought on from many complications, such as non-traumatic and traumatic causes [1]. The spinal column could become weakened due to various compressing pathologies, i.e., the expansion of blood products, cancerous disease, inflammatory abnormalities, growth of bone, or intervertebral disc within the constrained area of the fat-formed spinal epidural cavity and meninges [2]. Diagnostic measures are pivotal in assessing and treating non-traumatic spinal cord compression, emphasizing the critical roles of emergency physicians, neurosurgeons, and multidisciplinary teams in managing affected individuals [3].

The human spine is composed of 33 vertebrae. The 26 non-fused spine portions are isolated with cartilaginous intervertebral disks and tightly held by ligaments: the anterior longitudinal ligament and the posterior longitudinal ligament. Each neural foramen is enshrouded superiorly with a pedicle, immediately inferiorly by a disc space, posteriorly by facet joints, and anteriorly by the vertebral body [4].

The spinal epidural space, bordered anteriorly by the vertebral body and posteriorly by the dura mater, contains fat, arteries, and venous plexus. Notably, this space is more expansive in the thoracolumbar spine, which correlates with a higher incidence of spinal epidural abscesses in this area [5].

The most severe consequence of untreated spinal cord compression from any cause is irreversible neurological damage, including paralysis, difficulties in walking, sensory deficits, and loss of bladder and bowel control. Surgical complications after the spinal cord decompression could result in iatrogenic spinal cord and nerve root injury, durotomy with following cerebrospinal fluid leak, epidural hematoma, wound infection, and nonunion. These must be considered for the perceived benefits of operative decompression, with individual patient's age, comorbidities, duration, and severity of symptoms [6].

Acute paraplegia may occur in patients undergoing treatment for spinal cord compression due to the gradual blockage of arteries supplying the spinal cord, a situation more common in older individuals with atherosclerosis [7].

The compression spinal cord injuries are documented to be a typical complication of morbidity in patients who suffer from a spinal cord injury (SCI) [8]. Whether arising from traumatic events or non-traumatic conditions like cervical myelitis, compression injuries lead to significant clinical pain. Numerous animal studies have been conducted to investigate these injuries [9], although these studies often focus more on the immediate physical impact rather than the chronic nature of compression SCIs. Nontraumatic spinal cord injuries have been ignored by groups of scientists and have increased complications across all age groups [10]. Therefore, there is an urgent need to seriously assess the current animal models of compression SCI and their practical applicability as a method for clinically appropriate data that can facilitate morbidity and mortality of SCI to be minimized.

A review of both traditional and novel animal models for studying compression SCI highlighted techniques such as the clip, balloon, calibrated forceps, screw, solid spacer, expanding polymer, remote, weight drop, and strap methods [11]. These methodologies suggested that a large reliance on the use of laminectomy was to induce injury [12]. However, the age range of many studies is not representative of the elderly and young populations that generally experience pain from compression injuries. It is, therefore, essential to develop techniques that may reduce secondary complications of the surgeries, and an applicable model of the clinical treatments found in that treatments and interventions should be developed more specifically [13].

Compression injuries may be produced by multiple methods of applying force dorsally or laterally. Generally, methods of a compression injury are calibrated forceps, aneurysm clips, or directly placing weights onto the spinal cord. An advantage of using aneurysm clips is that they can exert well-controlled amounts of force [14]. Physically placing weights at the spinal cord's dorsal surface to simulate the amount of force requires the weight to be in place for 10 min, drastically increasing the surgery duration, which leads to inconsistencies in the movement of weight by the animal's respiration [15]. In mouse models, the small size complicates fixation in apparatuses designed for larger animals, like rats or rabbits, possibly leading to inconsistent injury types. Nevertheless, mice offer a substantial benefit for SCI research due to the availability of a wide range of transgenic strains [16].

The nervous system of an earthworm maintains a primitive brain of fused ganglia, a ventral nerve cord, and peripheral nerves. The peripheral nerves carry AP from the earthworm’s sensory cells to specific body parts, and coordinated responsive movements are well-established. For instance, when the sensory cells feel that the area outside its den is too hot, the earthworm will move to a different location so that its less important posterior area will face that direction. When the organism acquires new information that the environments outside are physically favorable, it resides with its head towards the surface [17].

Some AP parameters have been studied with cortical neurons exhibiting several spiking dynamics both in in-vivo and in-vitro experiments. Neural spikes or action potentials (APs) are

also observed in various shapes and forms. Statistical correlation between AP parameters and associated spiking behavior of a neuron is discussed in this article. Three fundamental parameters-width, height, and energy of an AP-along with spiking frequency and interspike interval (ISI) are extracted for 91 human cortical neurons selected from Allen Institute for Brain Science (AIBS) database. It has been shown that neurons firing narrow, short, and low-energy APs have higher spiking frequency compared to the neurons with wide and taller APs. For a rise in excitation, it has been presented that information gain for neurons firing wider spikes is less compared to information gain for neurons firing narrow spikes [18].

This study aimed to establish, through the use of an L. terrestris model, that simulated spinal cord compression could influence the characteristics of action potentials generated by electrical stimulation. Furthermore, it explored how these AP parameters could be altered through the application of pharmacological agents commonly encountered in daily life.

2. EXPERIMENTAL METHODS

2.1 Materials and Reagents

Data Science International (St. Louise, MO) manufactured our data acquisition system. The system consisted of the A/D matrix, ambient pressure monitor, transmitter, acquisition software, and data processing card with a PC that was all included for reliable waveform conditioning. The weight standard was bought from Harvard Apparatus (Holliston, MA). Canadian nightcrawlers such as L. terrestris were purchased from Dicks Sports (Paramus, NJ).

2.2 Data Acquisition System

The data acquisition system is very sensitive to any electric interference and static electricity. Even the switch function for powering light and moving around could cause accidental noises on the real-time monitor of the PC. The telemetry system was used to study safety pharmacology manufactured by implanting a DSI transmitter into small animals such as mice and rats. In this study, due to the subtle movements of L. terrestris, the experiment was accommodated by wiring the flexible electrodes of the transmitter into the subject's body. Our electrodes remained remarkably well-attached even when the subject was awakened mildly from anesthesia. Therefore, the telemetric monitoring system was readily controllable to execute this type of experiment due to the flexibility of the coiled wire electrodes. The electrical waveforms from the posterior spinal cord traveled into the transmitter through the electrodes. The transmitter then relayed that electrical information wirelessly to the receiver, which moved the information to the matrix that played the roles of multiplex and A/D converter so that the waveform could arrive at the software in the computer.

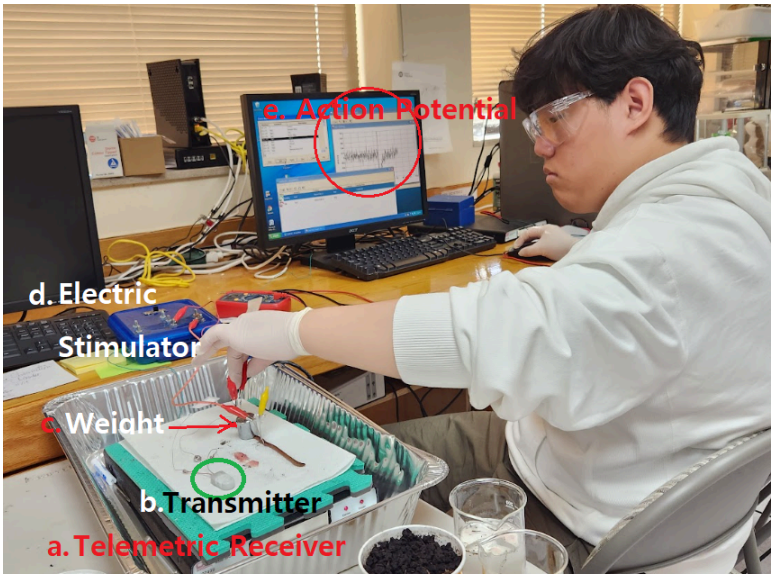

Fig. 1 demonstrates our experimental system for telemetric data acquisition. a: Telemetric Receiver, b: Transmitter, c: Weight Standard, 100 g, d: Electric Stimulator, e: Action Potential Display Monitor.

2.3 Data Acquisition Preparation Procedure

The study was carried out primarily by operating the diagnostics program to confirm the telemetry system was operating correctly. Once the diagnostic procedure was completed, the DSI-proprietary acquisition program was opened with event markers that were verified according to the study schedule of the day. The event markers should be supported to identify any experimentally significant events marked on the waveforms to find timely moments correctly after being restored for data analysis. After the software was running, its related parameters and functionalities should be thoroughly examined, for example to see the event marking tags in the study log button option.

2.4 Earthworm Anesthesia Procedure

An L. terrestris was randomly chosen and cleansed with water to take dirt from its body. Then, it was immersed in a 10% ethyl alcohol solution for about 6.0 ~ 9.0 minutes to make it unconscious. Once its deep anesthetization was confirmed with its no touching response and light reflex on the study pad, it was moved to the paper towel, and two dissection pins were pierced into the skin as the stimulation electrodes, positive at 9 cm posterior to the clitellum, while negative at 6 cm anterior. The positive electrode wired from the transmitter was inserted 2

cm posterior to the positive stimulation electrode, and the negative electrode was carefully pushed into the skin 2 cm anterior to the negative stimulation electrode.

2.5 Data Acquisition Procedure

The data acquisition telemetry system started recording the earthworm's action potential waveforms immediately after being inserted into the electrodes in the animal's body. The earthworm was electrically stimulated in 3 steps, with about 10.0 to 20.0-second intervals between each stimulation. The electrical stimulation was carried out with electrical potentials of 50.0 mV, 100 mV, then 150.0 mV. Once a set of electrical stimulation was generated for the earthworm for baseline waveform acquisition, the first weight, 10.0 grams, was placed on the skin just below the clitellum, which was approximately the middle point between the two sensing electrodes. After each stimulation, the weight was replaced with another weight as specified on the surface, and electric stimulations were given with or without drug injection. The identical procedures were repeated as scheduled in advance. Following each injection, three times of electric stimulations were given, and the action potentials were averaged to report the mean trend of the data.

2.6 Data Analysis

The waveform data was analyzed as below in Fig. 2. The waveform was played back from the study file using the Physiotat analysis software (Data Science International, MN), from which our event-marked segment of interest was exported to Excel, while the moment time of a data selection table was created in Microsoft Excel and typed data into the worksheet accordingly while identifying the segments of interest in the Physiostat analysis program. The time for each event marker was automatically uploaded into our data table when the action potential data set was imported. The definitions of the parameters are as follows: The distance between the two red arrows was defined as a response duration (RD). Fig. 2. presents a typical waveform and action potential peak point (PP) and lowest point as the nadir point (NP) in an action potential. For the wave width, the waveform baseline was traced carefully since the wave width was described as the distance between the starting point of uprise from the baseline to the peak and the ending point of uprise from the trough point to the baseline. All data were summarized with average and standard deviation. T-test was carried out when needed (SPSS, Sigmaplot, San Jose, CA).

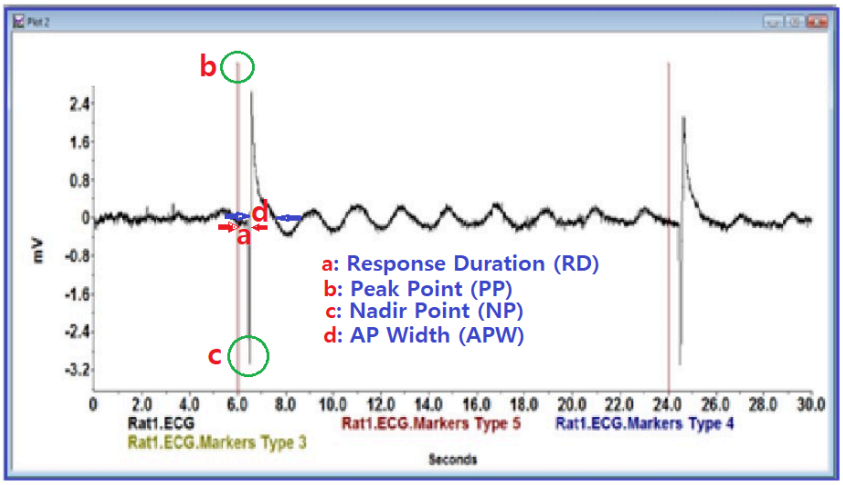

Fig. 2 presents a real-time segment of our waveform during our study after the electric stimulation and its subsequent output waveform of the action potential.

3. RESULTS AND DISCUSSION

3.1 Determination of Optimal Stimulation Potential for Action Potentials

3.1.1 50 mV Electrical Stimulation with Weight Changes

As a sensory initiation stimulus, it must be the first step of the study to confirm the optimal level of stimulation that could evoke the action potential with reproducible quantitation of the AP parameters. It has been known that this type of study usually produces biopotential data with high variability since the data comes from extremely low potentials. Further, our primary focus of the study was how much the parameters can be changed according to the weight increase pressed on the spinal cord of L. terrestris. This data was acquired with a 50 mV electrical stimulus. The first one we found was that the change profiles were highly correlated with polynomial functions with respect to the change of weights. Their R2 scattered from 0.7046 to 0.8785. Each parameter had unique characteristics in changing patterns. These regression numbers were calculated with the trendline functions in MS Excel. It looked like it was approaching a plateau in response duration and nadir point, while AP width and peak point showed consistent dependency on weight change.

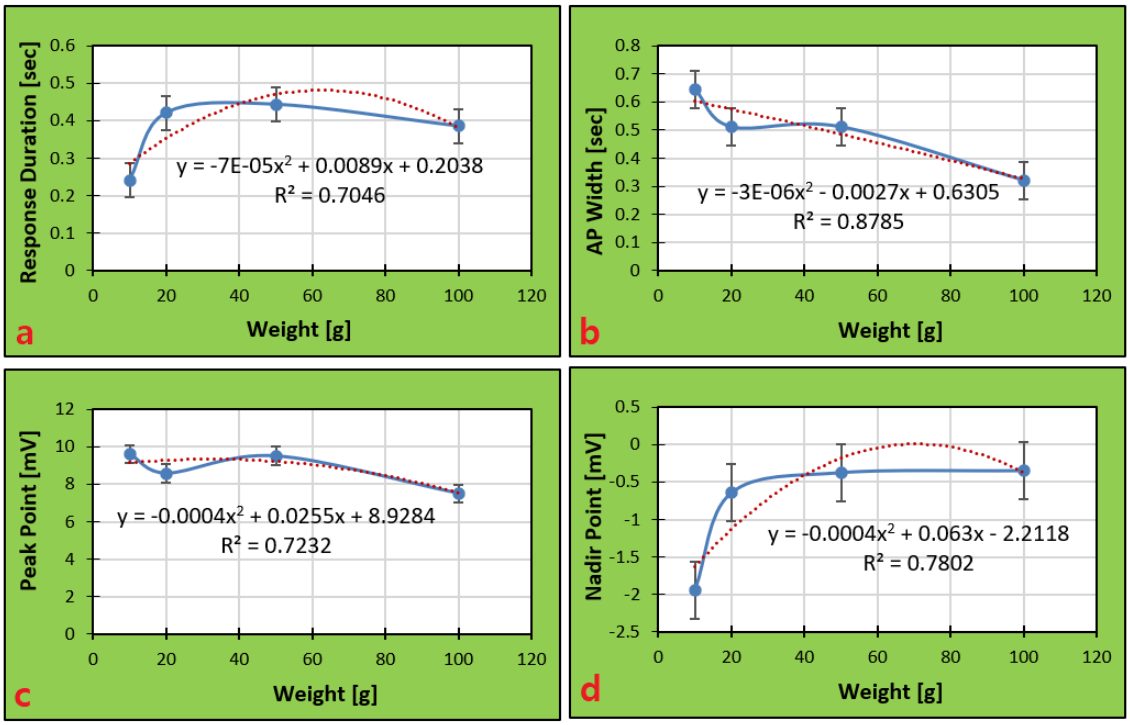

Fig. 3 presents the change of AP parameters by 50 mV electrical stimulation with respect to the standard weights placed on the nerve cord.

3.1.2 100 mV Electrical Stimulation with Weight Changes

Now, this data was acquired with a 100 mV electrical stimulus. It was apparent that response duration and nair point were changed with highly correlated polynomial patterns, while AP width and peak point were moderately followed by weight change. Their R2 scattered from 0.6164 to 0.9534. Each parameter had unique characteristics in changing patterns. Looking closely into the four cases, some reversal weights were important to the AP parameter changes. As seen in Fig. 4 below, the RD was increased, while PP and AP width were decreased after a plateau was reached. The ND is not very dependency on the weight of the animal's spine.

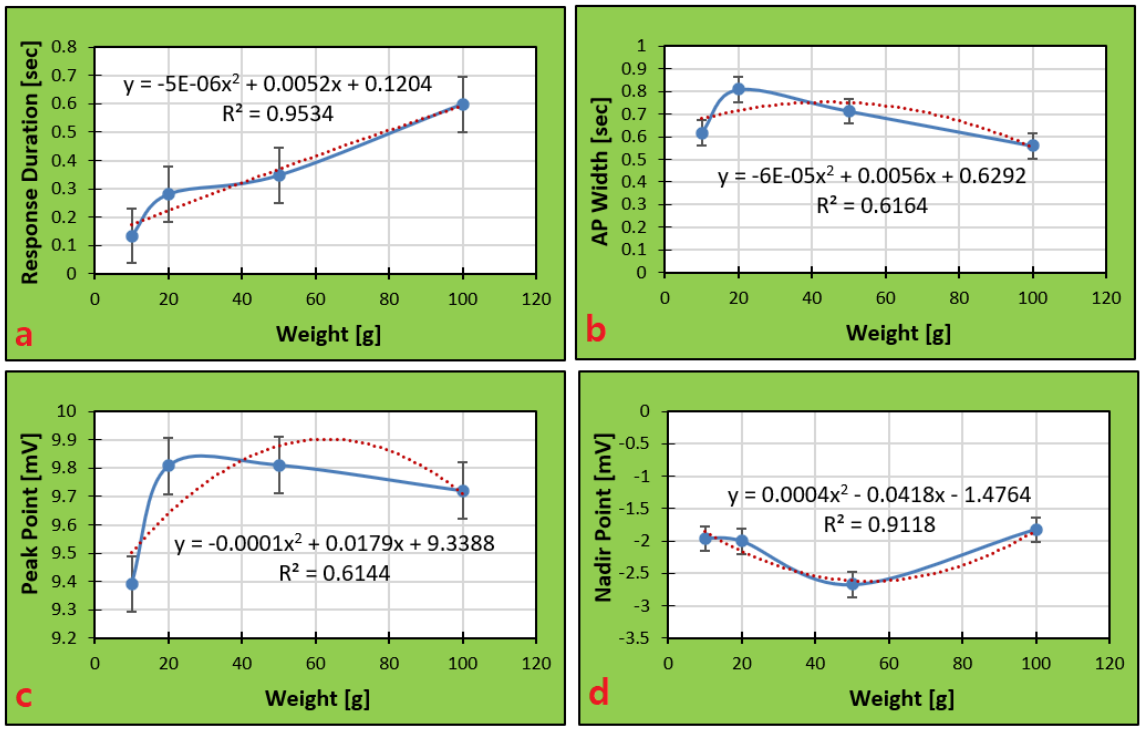

Fig. 4 presents the change of AP parameters by 100 mV electrical stimulation with respect to the standard weights placed on the nerve cord.

3.1.3 150 mV Electrical Stimulation with Weight Changes

This data was obtained with a 150 mV electrical stimulus. Their R2 scattered from 0.2952 to 0.9996. Each parameter had unique characteristics in changing patterns. In a quick glimpse, the AP width was the most poorly related to the changes in weight pressure, while other parameters remained highly correlated with the weight changes. In fact, the data looked reasonable for the amplified dispersion across the ranges, considering the magnitude of stimulated electrical potential to be unnecessarily high. When comparing the values as percentages of the largest and lowest data, the data moved 50 ~ 70%.

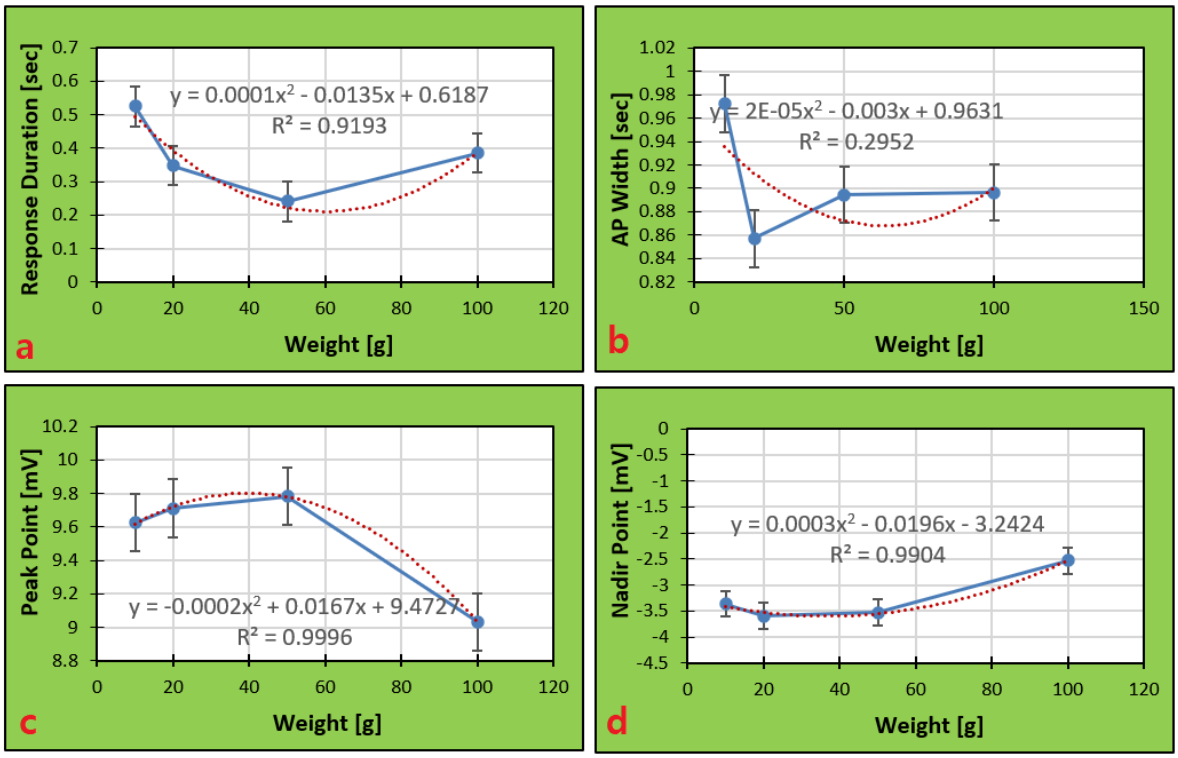

Fig. 5 presents the change of AP parameters by 150 mV electrical stimulation with respect to the standard weights placed on the nerve cord.

3.1.4 Combined the Three Simulations from Above

The figure below was created with the data of the three previous plots for choosing the most optimal electrical stimulation for further study. Reviewing the parameter profiles for the different electrical stimulations, it was then decided to study further with only 100 mV electrical stimuli since it generated more consistent data than other data groups. Each parameter had unique characteristics in changing patterns, as seen in the Figures. The changing patterns looked smoothly curved with a reversal point. Reviewing the parameter profiles for the different electrical stimulations, it was then found to study further with only 100 mV electrical stimulation since it generated more consistent data than other data groups.

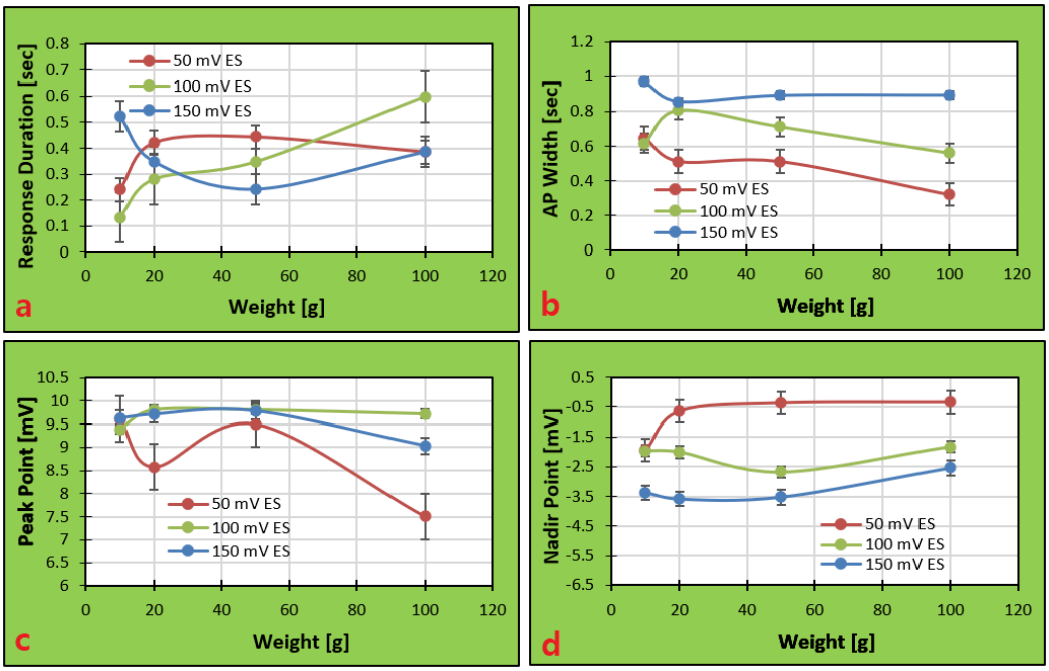

Fig. 6 presents the change of AP parameters at various electrical stimulations with respect to the standard weights placed on the nerve cord.

3.3 Parameter Change by Various Injections of Pharmacological Agents

3.3.1 Response Duration (RD) Change

Once an action potential is initiated at one point in the nerve cell, it propagates to the synaptic terminal region in an all-or-nothing fashion. The axon and the charge distributions would be expected to occur along the membrane of that axon. Positive charges exist outside the axon, and negative charges are on the inside. Now consider the consequences of delivering some stimulus to a point in the middle of the axon. If the depolarization is sufficiently large, voltage-dependent sodium channels should be opened. An action potential should be initiated, and it takes response duration to be sensed by the electrodes, where the changing potential is picked up.

Response duration was the time taken from the event marker to the AP starting point, which was read from the individual waveform after their raw data was retrieved from the acquisition software The results showed that the RD change from caffeine injection was less (-18.3%), while Tylenol and alcohol injection were greater (+20,9%, +32.7%), compared to the injection of saline, though no statistical difference existed ($P>0.05$). In fact, it looked reasonable since most physiological parameters are getting slow when intoxicated by alcohol and Tylenol, while shortened when too much is consumed in caffeine.

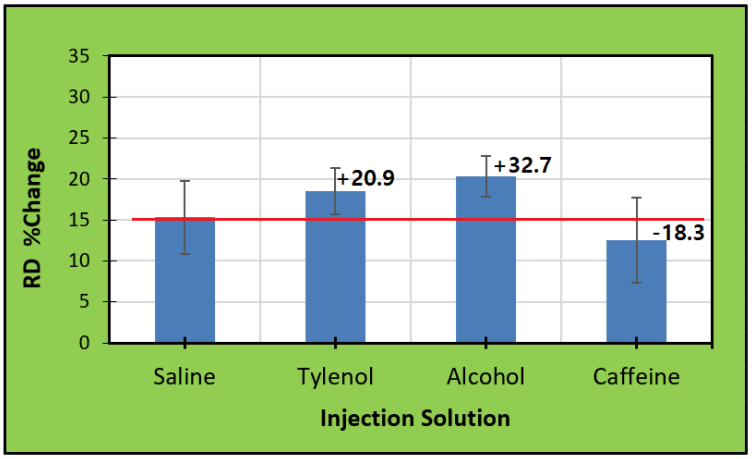

Fig. 7 illustrates the RD %Change for pharmacological administration (n=6). The numbers at the bar top are the percent difference compared to the saline RD % change.

3.3.2 Action Potential Width (APW) Change

In muscle cells, a typical action potential lasts about a fifth of a second. In plant cells, an action potential may last three seconds or more. The electrical properties of a cell are determined by the structure of its membrane. In this study, the action potential width was calculated by subtracting the AP ending point from the AP starting point. The time included the depolarization and repolarization and back to the resting potential. So, when there were any abnormal activities in the protein channels, the AP might be changed accordingly. Our data showed that APW became greater under the effects of Tylenol (72.2%) and caffeine (+111.1%), while smaller in caffeine, though larger than saline injection (+27.8%). The tendency was similar to the data previously we got as seen in Fig.8.

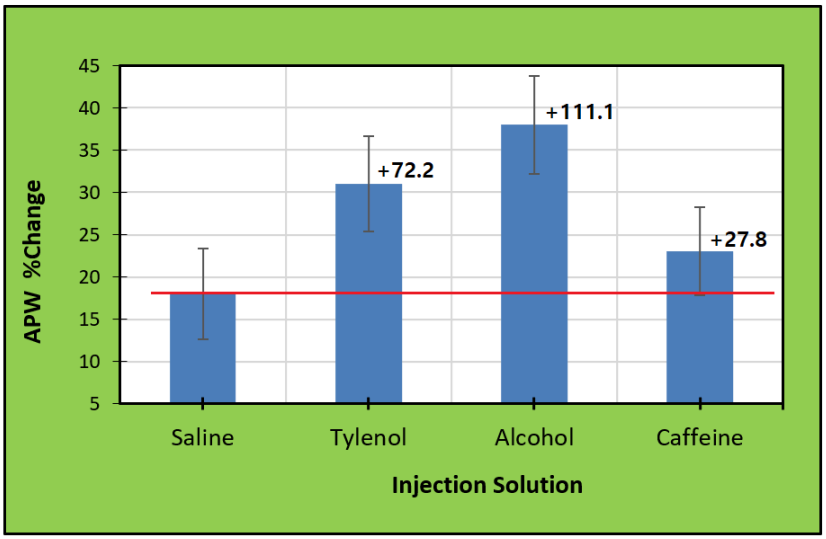

Fig. 8 illustrates the APW %Change for pharmacological administration (n=6). The numbers at the bar top are the percent difference compared to the saline APW % change.

3.3.3 Action Potential Parameter Peak Potential (PP) Change

The membrane potential starts out at approximately −70 mV at time zero. A stimulus is applied at time = 1 ms, which raises the membrane potential above −55 mV (the threshold potential). After the stimulus is applied, the membrane potential rapidly rises to a peak potential of +40 mV at time = 2 ms. And because the peak amplitude of the action potential depends on the value of the sodium equilibrium potential, the peak amplitude of the action potential would also decrease over time. Action potential width was calculated by subtracting the AP ending point from the AP starting point. The time included the depolarization and repolarization and back to the resting potential. So, when there were any abnormal activities in the protein channels, the AP might be changed accordingly. Our data demonstrated increases with the injection of the solutions, and the PP% changes were greater in caffeine, Tylenol and alcohol in order. Data looked more variable than that from other drug injections.

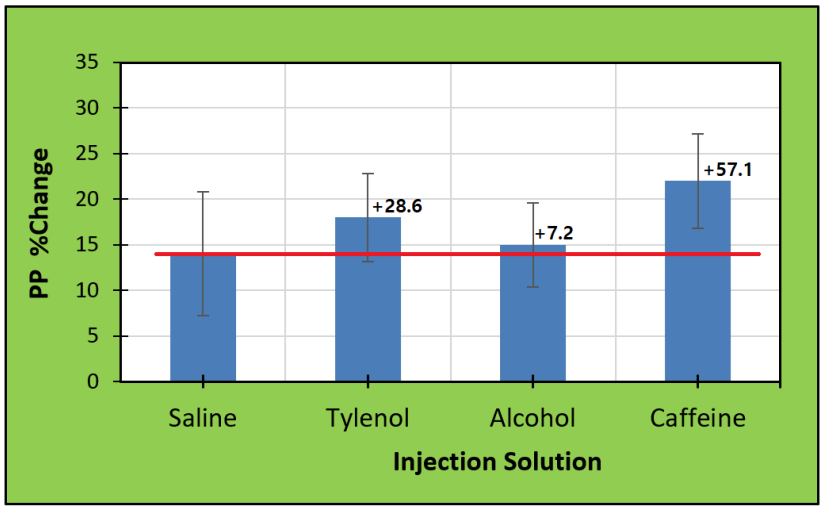

Fig. 9 illustrates the PP change by the pharmacological solutions (n=6).
The numbers at the bar top are the percent difference compared to the saline PP % change.

3.3.4 Action Potential Parameter Nadir Potential (NP) Change

The rapid influx of sodium ions causes the polarity of the plasma membrane to reverse, and the ion channels then rapidly inactivate. As the sodium channels close, sodium ions can no longer enter the neuron and are transported back out of the plasma membrane. Potassium channels are then activated, and there is an outward current of potassium ions, returning the electrochemical gradient to the resting state. After an action potential has occurred, there is a transient negative shift called the afterhyperpolarization. So, the NP can depend on various factors during back-to-resting potential. The nadir potential (NP) was read at the time point of the lowest potential during the course of the action potential. It showed that not much of a change in the magnitude of the NP, but they had variables as seen with standard deviation when injected with Tylenol (-16.7%), alcohol (-11.11%), and caffeine (-5.6%) as in Fig. 10 below.

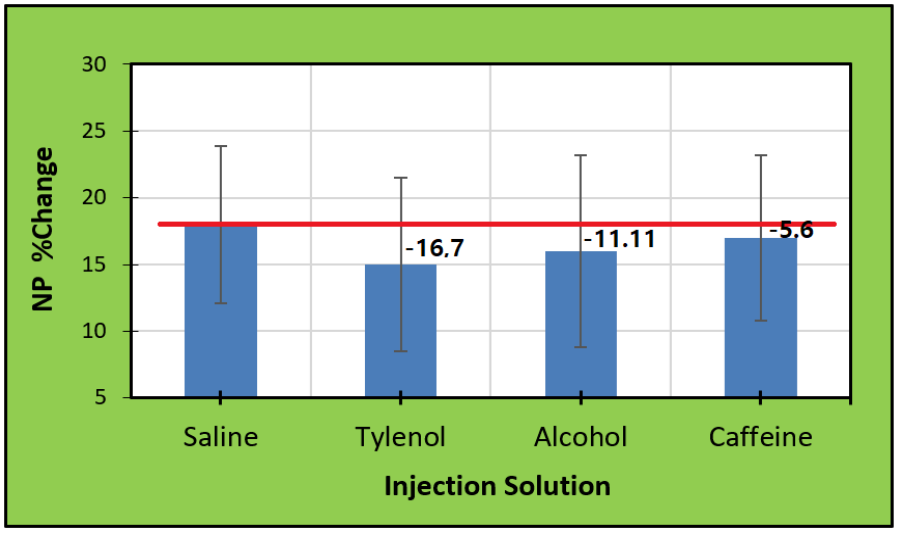

Fig. 10 illustrates the NP change by the injection of the pharmacological agents (n=6). The numbers at the bar top are the percent difference compared to the saline NP % change.

3.4 Summarized Results

The action potential parameters by spinal cord compression and pharmacological change were evaluated. At first, the AP parameters were changed with some variability to move their own characteristics. Still, they demonstrated similar profiles according to the change in pressing weight. For example, AP width and PP were increased, while RT and NP were decreased with the increase of the data. Likewise, the parameters change also showed unique profiles of change by the pharmacological injection.

4. CONCLUSION

Spinal cord compression is formed by a malignant tumor-generated pressure on the spinal cord. The Compression may be initiated anywhere around the spinal cord. Spinal cord compression may be generated by any pathological condition that brings pressure on the spinal cord, i.e., in case the vertebrae are physically damaged or pressed. Back pain is also sustained throughout the leg area for general complaints. Despite these serious issues, not many animal models have been established. This study investigated the impact on evoked potential parameters such as response duration (RD), peak potential (PP), action potential width (APW), and nadir potential (NP) to investigate any functional relationship for the standard weights placed on *Lumbricus terrestris*' body. The compression of *Lumbricus terrestris*' spinal cord by weight standards simulated the growing tumors in a confined spinal space. It was concluded that RP and NP were positively correlated, while PP and EPW were negatively correlated ($P<0.05$). The tendency of parameter impacts by the weights was shown to be consistent. Moderate changes were evident for all the parameters from the weight load on the spine. Further study might be continued to expound on detailed underlying mechanisms of the parameter profiles.

REFERENCES

1. Singleton, Jennifer M. “Spinal Cord Compression.” *StatPearls [Internet]*., U.S. National Library of Medicine, 13 Feb. 2023, www.ncbi.nlm.nih.gov/books/NBK557604/.
2. “Spinal Cord Compression.” *Johns Hopkins Medicine*, 8 Aug. 2021, www.hopkinsmedicine.org/health/conditions-and-diseases/spinal-cord-compression.
3. Kruger, Erwin A, et al. “Comprehensive Management of Pressure Ulcers in Spinal Cord Injury: Current Concepts and Future Trends.” *The Journal of Spinal Cord Medicine*, U.S. National Library of Medicine, Nov. 2013, www.ncbi.nlm.nih.gov/pmc/articles/PMC3831318/.
4. Choi, Young Kook. “Lumbar Foraminal Neuropathy: An Update on Non-Surgical Management.” The Korean Journal of Pain, vol. 32, no. 3, 1 July 2019, pp. 147–159, www.ncbi.nlm.nih.gov/pmc/articles/PMC6615450/, https://doi.org/10.3344/kjp.2019.32.3.147.
5. Gala, Foram B, and Yashant Aswani. “Imaging in Spinal Posterior Epidural Space Lesions: A Pictorial Essay.” *The Indian Journal of Radiology & Imaging*, U.S. National Library of Medicine, 2016, www.ncbi.nlm.nih.gov/pmc/articles/PMC5036327/.
6. Singleton, Jennifer M. “Spinal Cord Compression.” *StatPearls [Internet]*., U.S. National Library of Medicine, 13 Feb. 2023, www.ncbi.nlm.nih.gov/books/NBK557604/.
7. Epstein, NancyE. “Effect of Spinal Cord Compression on Local Vascular Blood Flow and Perfusion Capacity by Alshareef M, Krishna v, Ferdous J, Aishareef A, Kindy M, Kolachalama VB, et Al.” Surgical Neurology International, vol. 7, no. 26, 2016, p. 682, www.ncbi.nlm.nih.gov/pmc/articles/PMC5054644/, https://doi.org/10.4103/2152-7806.191077.
8. Hagen, Ellen Merete. “Acute Complications of Spinal Cord Injuries.” World Journal of Orthopedics, vol. 6, no. 1, 2015, p. 17, www.ncbi.nlm.nih.gov/pmc/articles/PMC4303786/, https://doi.org/10.5312/wjo.v6.i1.17.
9. Ridlen, Reggie, et al. “Animal Models of Compression Spinal Cord Injury.” *Journal of Neuroscience Research*, U.S. National Library of Medicine, Dec. 2022, pubmed.ncbi.nlm.nih.gov/36121155/.
10. Ge, Laurence, et al. “Traumatic and Nontraumatic Spinal Cord Injuries.” World Neurosurgery, U.S. National Library of Medicine, 15 Dec. 2017, pubmed.ncbi.nlm.nih.gov/29253698/.
11. Ridlen, Reggie, et al. “Animal Models of Compression Spinal Cord Injury.” *Journal of Neuroscience Research*, U.S. National Library of Medicine, Dec. 2022, pubmed.ncbi.nlm.nih.gov/36121155/.
12. Chen, Yuyue, et al. “Could Extended Laminectomy Effectively Prevent Spinal Cord Injury Due to Spinal Shortening after 3-Column Osteotomy? - BMC Musculoskeletal Disorders.” BioMed Central, BioMed Central, 17 Aug. 2023, bmcmusculoskeletdisord.biomedcentral.com/articles/10.1186/s12891-023-06751-w.
13. Wong, Arnold YL et al. “Low back pain in older adults: risk factors, management options and future directions.” Scoliosis and spinal disorders vol. 12 14. 18 Apr. 2017, doi:10.1186/s13013-017-0121-3
14. McDonough, Ashley et al. “Calibrated forceps model of spinal cord compression injury.” *Journal of visualized experiments : JoVE* ,98 52318. 24 Apr. 2015, doi:10.3791/52318
15. Manohar, Anitha et al. “Cortex-dependent recovery of unassisted hindlimb locomotion after complete spinal cord injury in adult rats.” eLife vol. 6 e23532. 29 Jun. 2017, doi:10.7554/eLife.23532
16. McDonald, Brandon Z., et al. “The Nanotheranostic Researcher’s Guide for Use of Animal Models of Traumatic Brain Injury.” Journal of Nanotheranostics, vol. 2, no. 4, Dec. 2021, pp. 224–68, https://doi.org/10.3390/jnt2040014.
17. “Molecular Expressions Microscopy Primer: Specialized Microscopy Techniques - Differential Interference Contrast Image Gallery - Earthworm Nervous Tissue.” Micro.magnet.fsu.edu, micro.magnet.fsu.edu/primer/techniques/dic/dicgallery/earthwormnervessmall.html.
18. Chakraborty, Ayan, et al. “Action Potential Parameters and Spiking Behavior of Cortical Neurons: A Statistical Analysis for Designing Spiking Neural Networks.” IEEE Transactions on Cognitive and Developmental Systems, 21 June 2022, ieeexplore.ieee.org/document/9802723/.